Technical Report *February 28, 2023*

Non-Invasive Blood Glucose Monitoring: A Validation of a Novel Sensor Compared to a Dexcom G6®

Dominic Klyve[1], Barry Shelton[2], Steve Lowe[3], Carl Ward[4], David Schwarz[4], Steve Kent[2]*

[1] Department of Mathematics, Central Washington University Ellensburg 98926, USA. klyved@cwu.edu
[2] Know Labs, Inc.
[3] Igor Institute, LLC
[4] Edge Impulse, Inc.

Abstract: This paper presents proof of concept for a new method to quantify blood glucose in vivo non-invasively using RF methods by means of training a model to predict readings of the Dexcom G6®, a popular continuous glucose monitor (CGM), as a proxy for BGL. The method uses a new type of sensing device that rapidly scans a wide band of RF frequencies. We further detail the data science techniques used to train a neural network model on our data to make our predictions. The trained model had a Mean Absolute Error of 25.8 mg/dL and a Mean Absolute Relative Difference (MARD) of 19.3%. We report other metrics of model success and discuss future directions of this work.

Keywords: glucose, blood glucose, non-invasive blood glucose monitoring, biomarkers, biosensors, radio frequency sensors, microwave sensors, point-of-care diagnostics, personalized medicine, neural network modeling.

1. Introduction

Diabetes Mellitus (DM) is a disease associated with high blood glucose levels (BGL) that has been estimated to affect over 500 million people worldwide. To reduce the risk of long-term negative health effects associated with DM, it is necessary to regulate BGL through medication or insulin injections [1]. To monitor BGL, portable measurement devices, which require a small drop of blood obtained from a pricked fingertip to be applied onto a test strip, are widely used by patients. This process is invasive and both incurs ongoing costs and creates biomedical waste. Depending on the severity of disease, up to 10 measurements a day may be needed, causing considerable discomfort. Furthermore, the contaminated consumables such as test strips and needles must be disposed of properly to avoid potential health risks associated with the spread of blood-borne diseases. Other patients use modern continuous glucose monitors (CGMs), though these involve the concomitant pain of CGM probe insertion and cost of regular replacement. The need for a portable, non-invasive, point-of-care tool that accurately measures BGL remains.

Various methods of measuring BGL non-invasively are being explored by researchers in the field of biosensors, with the Radio Frequency (RF)/microwave sensing technique being one of the more promising approaches [2]. This technique uses an RF sensor to measure the change in the dielectric properties of blood caused by a change in BGL, and thus serves as a biomarker for glucose in vivo [3]. RF sensing methods have a clear advantage over optical sensors because optical methods have shown performance problems on people with high melanin skin [4].

Glucose biosensors have existed for over half a century. Broadly, they can be classified into two groups: electrochemical sensors that rely on direct interaction with an analyte and electromagnetic sensors that leverage antennas and/or resonators to detect changes in the dielectric properties of the blood. Every commercially available glucose biosensor that has been approved for human use is invasive in some way, with the concomitant environmental waste, cost to the user, and in some cases human morbidity. Many researchers have expressed hope that the next generation of these types can lead to a non-invasive blood glucose sensor [5].

There has been an increasing interest in recent years in using resonators or antennas transmitting in the microwave range to detect glucose in aqueous solution, in an effort to exploit its dielectric properties. Largely focused on the 1 - 6GHz range, these have included both devices that work on a specific frequency [6]–[12] and those that employ a range of frequencies [13]. Tests have demonstrated that there seems to be promise in this approach, though none of the tests to date have been sufficiently precise to be of clinical use [14]. The field of RF sensing has been focused largely on in vitro studies [6]–[8], [10], [11], [14]–[21], some of which have made use of vascular phantoms to mimic human tissue [7], [9], [22], [23] with far fewer in vivo studies conducted over the past fifteen years[24]–[31], largely because in vivo tests of RF bio-sensors pose a unique set of challenges.

The primary difficulty of using microwaves to sense BGL is establishing the correlation between effective permittivity and BGL [32]. The hurdles in understanding this correlation are 1) sensitivity and 2) selectivity [33]. Changes in the dielectric properties of tissues because of changes in BGL are extremely small, so creating a sensor capable of measuring these minute changes in living subjects has proven to be a challenge, because alongside sensitivity comes susceptibility to both noise and interference [6]. Similarly, selectivity is a problem, because the RF waves must penetrate skin, fat, and vascular layers–all of which have different dielectric properties–before reaching blood, and therefore signal post-processing is necessary to reduce interference from the waves being influenced by these other tissues.

Related research has focused on statistical and algorithmic development for the forecasting of BGL via post-processing of the signal. Researchers have employed machine learning techniques

to predict future blood glucose levels based on recent CGM readings using autoregressive models (ARMs) [34], neural networks (NN) [35], hybrid deep-learning models [36], multitask learning models [37], support vector regression [38], Extreme Gradient Boosting (XGBoost) [39], and deep ensemble models [40]. These models have had varying degrees of success, and are generally able to predict future glucose levels to an accuracy that is better than a baseline model; moreover, these models continue to improve as new algorithmic developments are made.

This paper presents proof of concept for a new method to quantify blood glucose non-invasively using RF methods by means of training a model to predict readings of the Dexcom G6®, a popular continuous glucose monitor (CGM), as a proxy for BGL. We describe a new type of sensing device that rapidly scans through a wide band of RF frequencies and records values detected of each frequency over a period of time. We further detail the data science techniques used to train an NN model on our data to make our predictions. This is the first in a planned series of studies in which we will continue to improve sensor characterization, data collection, and algorithm refinement with larger numbers of individuals.

2. Materials and Methods

2.1. Study Design

An observational study design was used in which data were collected every weekday during a 16-day period in the second half of July 2022. Data were simultaneously collected from the prototype device and a reference device during each testing session. To reduce variability in the data, a single individual (the "subject") was used for all tests. The subject was a 25–35-year-old female in good health. One test was performed each day, making a total of 11 tests. In order to minimize interference in the RF frequencies employed by the antenna, a location was selected in a remote research station in Yucca Valley, California in which there were minimal wi-fi, Bluetooth, or other signals. Efforts also were made to limit these signals in the local testing area.

2.2 Prototype Device

2.2.1. RF Sensor

The sensor employed in this study was the patented Know Labs Bio-RFID device, which consists of a Printed Circuit Board Assembly (PCBA) that generates RF signals and measures received power after passing those signals through an Antenna Array. Figure 1 shows an engineering diagram of the sensor and antenna array. Although not all available frequencies were used in this study, the sensor can generate RF signals that can range from just over 100 MHz to just over 4000 MHz. There is a transmit (Tx) amplifier to boost the signal, and then the RF signal is

routed through a switch matrix that allows for it to be sent to any one of the four supported antenna elements, or optionally through an onboard fixed-attenuation path called the Calibration Path that allows the system to test itself and provide a known benchmark.

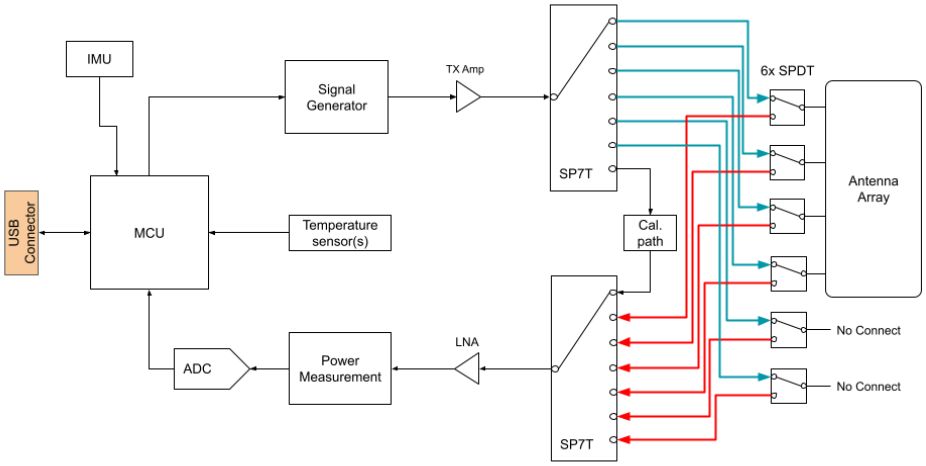

Figure 1: System architecture diagram of Know Labs Bio-RFID™ sensor

The same switch matrix also establishes the receive (Rx) path, where one of the four supported antenna elements (or the Calibration Path) is chosen to receive the transmitted signal. Once through the switch matrix, the signal is amplified with a Low Noise Amplifier (LNA) to set it in the appropriate range of the power measurement circuitry, which translates the received RF signal's power into a voltage output that can be sampled by the onboard Analog to Digital Converter (ADC).

These digitized values are accumulated in the firmware of the Microcontroller Unit (MCU), which is responsible not only for data collection but also controlling the whole system. The MCU accumulates samples during a dwell, which is defined as the period of time that the Signal Generator is active at a specific frequency, and then averages those samples to provide a single power measurement value per dwell over the device's USB connector. The system is also equipped with an onboard Inertial Measurement Unit (IMU) to detect motion and a thermometer to compensate for any temperature-related signal drifts.

2.2.2 Characteristics of the Sensor

The initial sensor antenna design used a single antenna element or a pair of transmit and receive elements, with design topologies derived from common narrow- and broad-band radiating structures (loops, monopoles, patches, spirals, etc.). Through experimentation, the system's best results were associated with "loosely coupled" structures. These are structures that, in air, had a nominal average value of transmission coefficient that was not "too strong" due to

large fringing- or near-fields, which made them highly susceptible to dielectric loading effects when exposed to a possible analyte. More designs were created based on this principle with the aid of finite element modeling (FEM) simulation tools and subjected to fast design/test/verify cycles with the use of rapid prototyping equipment.

This work led to the current instantiation of the Know Labs Bio-RFID sensor, which uses an array of antenna elements. These elements are not designed to radiate efficiently into free space, nor are they designed for any specific resonant frequency, though the system does display several resonant modes. Instead, they are intended to provide a mechanism for RF fields to be capacitively coupled from a selected transmit element to a selected receive element. The elements are spaced in a linear array, and the selection of transmit and receive elements depends on the relative element positioning that works best for the target analyte under test.

The RF PCBA effectively measures the Antenna Array's transmission coefficient, or S_{21} in scattering parameter terms, over its frequency of operation. For the Antenna Array, the measured S_{21} response varies widely depending on the specific analyte's dielectric properties. This results in a pair of effects that we can observe in the S_{21} measurement over frequency; namely, the aforementioned resonant frequencies move to new frequencies, and the overall received power also varies.

2.2.3 Safety of the Sensor

Because the device emits RF waves into the user's bodily tissue, it is critical to determine whether the amount of radiation absorbed by the user's body remains within safe limits. Specific Absorption Rate (SAR) testing of the device was done at an independent and certified laboratory in July of 2022 to determine the SAR level for specific frequencies over 1 gram of tissue. Table 1 shows the results of those tests.

Table 1: SAR values across a range of frequencies

FREQUENCY (MHz)	**W/Kg**
500	0.046
650	0.042
850	0.083
920	0.059
1900	0.042
2300	0.106
2450	0.065

As documented in US CFR Title 47, Chapter I, Subchapter A, Part 1, Subpart I §1.1310 [41], the generally accepted SAR for occupational exposure is a peak spatial average SAR of 8 W/kg, averaged over any 1 gram of tissue (with a cube shape). The accepted peak spatial-average SAR for the general public is 1.6 W/kg. The SAR levels generated by the sensor were well below these values. As seen in Table 1, the maximum SAR measured on the sensor was 0.106 W/kg. A more specific analysis that splits the frequencies of the sweep into smaller intervals and bounds each interval with the greater of its two endpoint values suggests that the average SAR over a seven-second period (six seconds of scan plus a one-second pause) is closer to 0.07 W/kg.

2.3 Reference Device

The Dexcom G6® is a continuous glucose monitor (CGM) device that uses interstitial fluid glucose levels as a proxy for BGL. The values from the Dexcom G6® device served as the response variable (the "labels") in our study, and we consider these to be a proxy for BGL throughout. The Dexcom G6® was chosen after a series of internal tests evaluating several options to collect reference data, including the Freestyle Libre (Abbot Diabetes Care, Alameda, California, USA) CGM and finger sticks (Accu-Chek® Guide, Roche Diabetes Care, Indianapolis, IN, USA), in which the Dexcom G6® data appeared to be most consistent and stable. The Dexcom G6® also is generally recognized as the industry leader in diabetic CGM.

2.4 Study Protocol

Each test ran for up to four hours and followed a similar procedure. The subject sat in a chair and placed left and right forearms on the prototype antennae. The subject was fitted with a Dexcom G6® (Dexcom, Inc., San Diego, California, USA) affixed to the posterior of the left arm to track interstitial glucose levels. To ensure optimal accuracy, the Dexcom G6® was inserted at least 24 hours before testing. After the first Dexcom G6® sensor expired, it was replaced with a new one in the same location. Efforts were made to minimize any body movement of the subject throughout the course of the test.

During 10 of the tests, the subject consumed 37.5 grams of liquid D-Glucose. D-Glucose was administered orally by drinking half of a 75 gram container of Azer Scientific Glucose Tolerance Test Beverage 30 minutes after the test began. During the following 2-3 hours, the subject's glucose levels rose and then fell. The test was stopped after the subject's Dexcom G6® values returned to their "baseline" for 30 minutes. We also conducted a single test in which the subject did not consume D-glucose, but remained on the devices for three hours.

2.5 Data Collection

Prototype data were collected on a continuous basis, using sweeps across the 500 MHz – 3000 MHz range at 1 MHz intervals, collecting values at 2501 frequencies on both the right and left arms, resulting in 22 datasets. A full sweep of these frequencies took approximately seven seconds, including a one second pause between sweeps. Over a typical 3-hour test, just over 1500 sweeps are performed. Each of our 22 tests thus collected approximately 3.8 million pieces of data. For the reference data, the Dexcom G6® iPhone application recorded glucose values from the reference device every five minutes for the entire duration of the test; these values were manually entered into a data table that was later used to label the larger datasets.

3. Data Analysis

Feature generation techniques were developed with custom signal processing routines in a Python v3.10.9 environment with Numpy v1.24.1, Pandas v1.5.3, SciPy v1.10.0 and scikit-learn v1.2.1 packages, and then hosted and used to process the raw data in the Edge Impulse platform. After feature generation, we employed regression techniques from the generated features to the Dexcom G6® CGM readings using Python v3.8.10 with TensorFlow v2.7.0, NumPy 1.21.4 and scikit-learn v1.1.1 packages.

3.1 Data Preparation

3.1.1 Feature generation

The 2501 features of this data were smoothed using a Savitzky-Golay filter with window length of 2000, polynomial order of 4, and derivative order of 1 (Savitzky 1964). Filter windows past the signal boundary were padded by repeating the nearest sample value. Finally we standardized the features by removing the mean and dividing by standard deviation per sample and then used Gaussian Random Projection to reduce the feature space to 256 [42], [43]. The resultant 256 features were computed for each sample and then aggregated before being used as input for machine learning.

3.1.2 Machine learning

The data described in Section 2.5 were labeled with the result of the Dexcom G6® reading at each time point. From the raw dataset, five separate randomized train/validation splits were generated, each with a different random seed, with two held-out samples per split to use for testing. Each split was then independently trained and evaluated.

In order to establish a baseline model to improve upon we chose to take the mean of the training set labels. This is analogous to taking a random label in a machine learning classification problem.

After cross-validation, we searched for suitable NN architectures and hyperparameter settings. Each algorithm was compared to the baseline (data not shown) and we selected the best-performing model based on the smallest validation error. The top-performing model consisted of two blocks each with a one-dimensional convolution layer followed by a pooling layer and finally a dropout layer (Figure 2). The final layer is a single neuron which was trained to predict the value from the DexCom® at each time point.

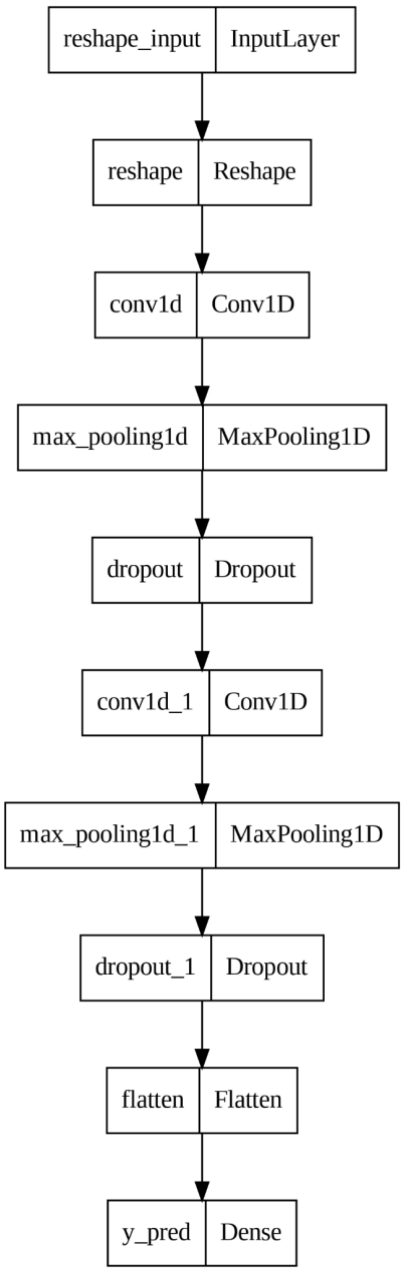

Figure 2: Architecture of the NN model

3.1.3 Model Testing and Statistical Analysis

After the NN was trained, we applied it to the test data, which had been withheld from the model up to this point. For each time point, the NN predicted the Dexcom G6® reading based on the data collected by the sensor, after which it was compared to the value from the Dexcom G6® device. The mean absolute error (MAE) was calculated for each data point. These values were calculated separately for each of the five folds (see Table 1). The MAE for the folds was then calculated. We also computed the mean absolute relative difference (MARD) of each prediction, defined as absolute error divided by the value of the Dexcom G6® reading.

In addition to calculating the MAE, we also calculated a binary measure of success. A prediction is said to be within threshold to the Dexcom G6® value if either: the prediction is within 15% of the reference value for blood sugars over 70 mg/dL; or the prediction is within 15 mg/dL for blood sugars below 70 mg/dL. These threshold values are modeled after FDA limits for accuracy in new blood glucose monitors. Statistical significance of differences in means was calculated using two-sample t-tests.

4. Results

4.1 Algorithm Performance

For each of the 20 datasets collected during a test in which glucose was consumed, we compared the Dexcom G6® values with three sets of values calculated for this study: the value of the baseline model, the predictions of the model when that dataset was in the training data, and the predictions of the model when the dataset was in the test data. Results are shown in Figure 3.

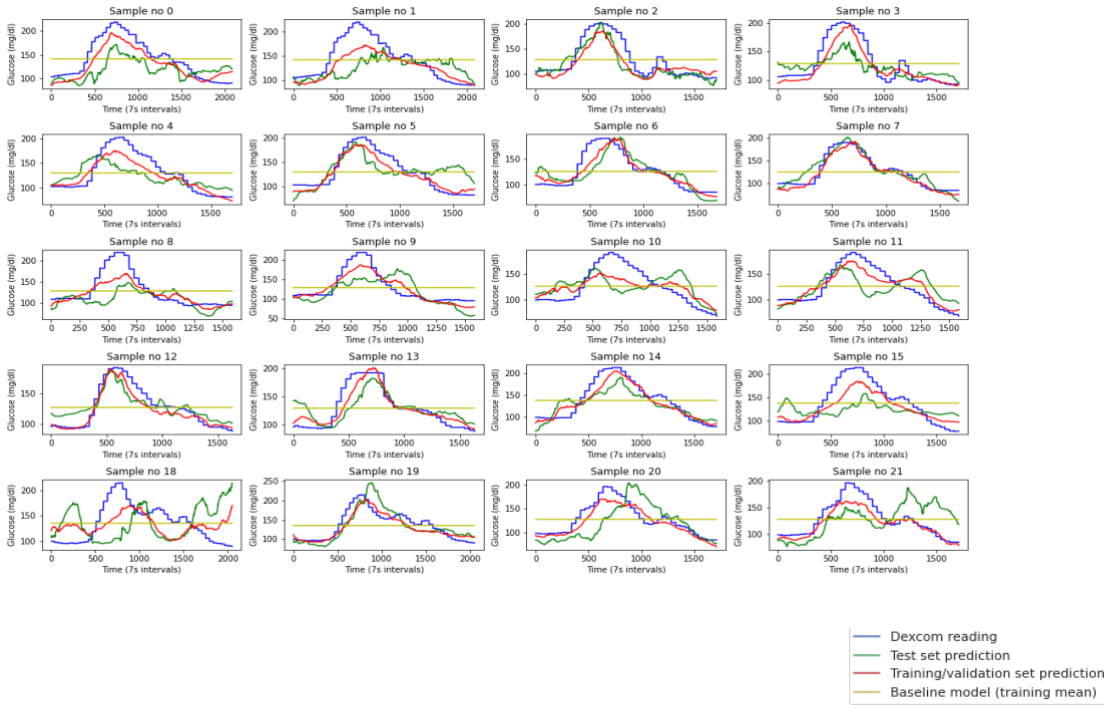

Figure 3. Results predicted by the NN and the base model (for both test and validation) of each sample, plotted with the Dexcom G6® readings across time. (Note that samples 16 and 17 were left out of this figure because the participant did not consume glucose in these two data sets.)

Summary data regarding model accuracy are given in Table 2, which reports the MAE of the baseline and trained models for both the train/validation data and test data for each fold.

On the training and validation set, the baseline model had an MAE with a 95% confidence interval of 32.98 ± 1.098. The NN performed significantly better ($t=19.36$, $p<0.001$), with an MAE of 15.49 ± 3.80.

The baseline model had similar performance on the training and test data. On the test data, the MAE for the baseline 'model' was 32.87 ± 3.37. The NN again performed significantly better, with an MAE of 25.80 ± 10.07 ($t=2.91$, $p < 0.05$).

Table 2. Mean absolute error (mg/dL) of the NN model and the Baseline model for the training+validation data and test data for each fold and mean and standard deviation (std) values across all folds.

	Training and Validation Dataset		Test Dataset	
Fold number	NN Model	Baseline 'model'	NN Model	Baseline 'model'
0	13.63	32.25	25.66	34.05
1	18.04	32.81	19.93	33.06
2	15.73	33.15	27.22	33.59
3	16.53	32.90	22.66	33.78
4	13.50	33.78	33.52	29.86
mean	15.49	32.98	25.80	32.87
std	1.94	0.56	5.14	1.72

Additionally, we found that 71% of values in the validation data and 46% of predictions on held-out test data were within threshold (as defined in Section 3.1.3). In the baseline model, by comparison, 25% of predictions in the test data were within threshold.

Finally, the relative errors of the NN model are given for each fold and across all folds in Table 3.

Table 3. MARD of the NN model for the test data

Fold number	Relative error of NN model (%)
0	17.46
1	16.46
2	20.33
3	17.04
4	25.85
Mean	19.3%

5. Discussion

In this study we present the results of an n-of-1 study design to assess the potential for using a novel RF-sensor to quantify blood glucose continuously and non-invasively, with the output of a Dexcom G6® CGM as a proxy for the measurement of blood glucose.

We describe the development of a new method that combines novel aspects of data collection utilizing the Bio-RFID sensor and Machine Learning techniques. Part of the novelty comes from the study design itself. Data were continually collected over a 2-3 hour period, sampling thousands of frequencies during every six-second sweep. Our model thus had access to several million datapoints for each dataset. Varying dielectric responses in different frequencies give the neural network model a more nuanced window into the system being scanned, and this may have mitigated some of the limitations of our small sample size.

Another way in which this study is different from previous efforts is related to the sensor itself. Typically, antennas in most communication systems are designed to radiate efficiently into free space, and as such, are typically designed to be resonant structures with a specific frequency of operation and radiation pattern in mind. The Bio-RFID antenna used in this study, however, is not designed to radiate signals; instead, it is an array of elements loosely coupled to each other, where each element is located primarily in the near field of another element in the array. The loosely coupled aspect means that the elements are neither spaced too close together nor too far apart. This lets the fields between them occupy the space in "front" of the array, meaning that the material that is placed in front of the array has a significant impact on how the fields behave, and thus on the coupling between the elements. Additionally, because the system operates over a broad frequency range, designing for a specific resonant frequency is not necessary, and designing for efficient coupling of fields into free space for the purposes of propagation is actually contrary to the system's goals of coupling energy from one element to another through a material medium.

By combining information from all frequencies collected by the sensor, the resulting NN model demonstrated an error that was significantly smaller than a baseline model. This is especially promising given the limited tests available for this pilot study. Neural network models thrive on large amounts of data, and the efficacy of the model discussed in this work based on only 11 tests yielding 22 data sets is encouraging.

Figure 3 shows how well each of the datasets was tracked by the model over time. Visually, one can see that the performance of the model varied significantly depending on the sample. Encouragingly, some of these samples were modeled extremely closely in both the training and test sets, while others showed strong variation from the actual values. This may suggest underlying environmental or physiological differences in these tests.

We also find the accuracy (as measured by size of error) of the predictions in this n-of-1 study are quite encouraging. A clinically useful non-invasive blood glucose sensor should make predictions within threshold (see Section 3.1.3) 95% of the time. With a MARD of 19.3%, we have begun to move toward that goal. Additionally, 46% of predictions on the test data were within threshold, which provides a floor against which to measure future work.

In the future, we anticipate collecting data from multiple participants, and we will continue to refine our data preparation and machine learning methods to hone our model further.

5.1 Limitations of the Current Study

5.1.1 Overfitting

This pilot study of the efficacy of the Bio-RFID sensor has several limitations. Perhaps the most obvious is that it was conducted on a single individual (n-of-1), which limits any claim of generalizability. At the same time, this lack of diversity restricted the ability of the model to be trained. We are in the process of executing additional studies with larger sample sizes to build on these results. In analyzing the performance of the algorithm, there is clear overfitting to the validation samples in each randomized split that was tested. In each case, performance on the test data was significantly poorer than on the training data. We expect that future work on larger numbers of participants will better be able to capture human variation and will reduce this difference.

5.1.2 Environment

The environment provided another limitation. We know based on extensive experience with the sensor that it is highly sensitive to electromagnetic interference, including Bluetooth and Wi-Fi signals. While reasonable attempts were made to limit exposure to these, we cannot rule out small disruptions in the data caused by such signals.

5.1.3 Reference Device

The authors want to clearly state that we make no claim to have predicted a biological event (e.g. a change in BGL). All models were trained to predict the values produced by the Dexcom G6® and were assessed on their ability to do so. The Dexcom G6® was chosen as the most practical for the study design and to achieve the high sampling frequency needed. However, we do not claim this is the gold standard for blood glucose and acknowledge this method has limitations, in particular that it is sampling interstitial fluid and not blood directly. We are exploring alternative reference measures for future work.

Conclusions

In this work, we describe the results of a study that we hope will lead to a new method of quantifying blood glucose. We utilized a novel type of sensing device combined with machine learning techniques to build an NN model to predict Dexcom G6® readings as a proxy for BGL on one individual over a series of tests. These tests, lasting 2-3 hours, involved gathering regular data from the Dexcom G6®, along with several million values collected by the sensor. The data were split between test and training sets; the model was trained on the latter and tested on the former. The model shows promising results, with a mean absolute error on the test set of 25.80 mg/dL (MARD 19.3%). Future work will expand data collection to multiple individuals in order to refine this model.

Author Contributions: Conceptualization, D.K. and S.K.; Methodology, D.K., S.L., C.W., D.S., S.K.; Software, S.L, C.W., D.S.; Validation, S.K.; Formal Analysis, D.K., C.W., and D.S.; Investigation, S.K.; Resources, S.L., S.K.; Data Curation, C.W., D.S.; Writing – Original Draft Preparation, D.K., B.S., S.L., C.W., D.S, S.K.; Writing – Review & Editing, D.K., B.S., S.L., C.W., D.S; Visualization, S.L., C.W., D.S.; Supervision, S.K.

Funding: This research received no external funding.

References:

[1] "Textbook of Diabetes, 5th Edition | Wiley," Wiley.com. https://www.wiley.com/en-us/Textbook+of+Diabetes%2C+5th+Edition-p-9781118912027 (accessed Feb. 23, 2023).

[2] L. Tang, S. J. Chang, C.-J. Chen, and J.-T. Liu, "Non-Invasive Blood Glucose Monitoring Technology: A Review," Sensors, vol. 20, no. 23, Art. no. 23, Jan. 2020, doi: 10.3390/s20236925.

[3] C. Jang, H.-J. Lee, and J.-G. Yook, "Radio-Frequency Biosensors for Real-Time and Continuous Glucose Detection," Sensors, vol. 21, no. 5, Art. no. 5, Jan. 2021, doi: 10.3390/s21051843.

[4] A. M. Cabanas, M. Fuentes-Guajardo, K. Latorre, D. León, and P. Martín-Escudero, "Skin Pigmentation Influence on Pulse Oximetry Accuracy: A Systematic Review and Bibliometric Analysis," Sensors (Basel), vol. 22, no. 9, p. 3402, Apr. 2022, doi: 10.3390/s22093402.

[5] C. G. Juan, B. Potelon, C. Quendo, and E. Bronchalo, "Microwave Planar Resonant Solutions for Glucose Concentration Sensing: A Systematic Review," Applied Sciences, vol. 11, no. 15, Art. no. 15, Jan. 2021, doi: 10.3390/app11157018.

[6] T. Yilmaz, T. Ozturk, and S. Joof, “A Comparative Study for Development of Microwave Glucose Sensors”.

[7] J. Vrba, J. Karch, and D. Vrba, “Phantoms for Development of Microwave Sensors for Noninvasive Blood Glucose Monitoring,” International Journal of Antennas and Propagation, vol. 2015, p. e570870, Mar. 2015, doi: 10.1155/2015/570870.

[8] V. Turgul and I. Kale, “Permittivity extraction of glucose solutions through artificial neural networks and non-invasive microwave glucose sensing,” Sensors and Actuators A: Physical, vol. 277, pp. 65–72, Jul. 2018, doi: 10.1016/j.sna.2018.03.041.

[9] T. Yilmaz, R. Foster, and Y. Hao, “Broadband Tissue Mimicking Phantoms and a Patch Resonator for Evaluating Noninvasive Monitoring of Blood Glucose Levels,” IEEE Transactions on Antennas and Propagation, vol. 62, no. 6, pp. 3064–3075, Jun. 2014, doi: 10.1109/TAP.2014.2313139.

[10] H. Choi et al., “Design and In Vitro Interference Test of Microwave Noninvasive Blood Glucose Monitoring Sensor,” IEEE Transactions on Microwave Theory and Techniques, vol. 63, no. 10, pp. 3016–3025, Oct. 2015, doi: 10.1109/TMTT.2015.2472019.

[11] N.-Y. Kim, K. K. Adhikari, R. Dhakal, Z. Chuluunbaatar, C. Wang, and E.-S. Kim, “Rapid, Sensitive and Reusable Detection of Glucose by a Robust Radiofrequency Integrated Passive Device Biosensor Chip,” Sci Rep, vol. 5, no. 1, Art. no. 1, Jan. 2015, doi: 10.1038/srep07807.

[12] K. K. Adhikari and N.-Y. Kim, “Ultrahigh-Sensitivity Mediator-Free Biosensor Based on a Microfabricated Microwave Resonator for the Detection of Micromolar Glucose Concentrations,” IEEE Transactions on Microwave Theory and Techniques, vol. 64, no. 1, pp. 319–327, Jan. 2016, doi: 10.1109/TMTT.2015.2503275.

[13] B. Freer and J. Venkataraman, “Feasibility study for non-invasive blood glucose monitoring,” in 2010 IEEE Antennas and Propagation Society International Symposium, Jul. 2010, pp. 1–4. doi: 10.1109/APS.2010.5561003.

[14] C. Jang, J.-K. Park, H.-J. Lee, G.-H. Yun, and J.-G. Yook, “Non-Invasive Fluidic Glucose Detection Based on Dual Microwave Complementary Split Ring Resonators With a Switching Circuit for Environmental Effect Elimination,” IEEE Sensors Journal, vol. 20, no. 15, pp. 8520–8527, Aug. 2020, doi: 10.1109/JSEN.2020.2984779.

[15] V. Turgul and I. Kale, “Characterization of the complex permittivity of glucose/water solutions for noninvasive RF/Microwave blood glucose sensing,” in 2016 IEEE International Instrumentation and Measurement Technology Conference Proceedings, May 2016, pp. 1–5. doi: 10.1109/I2MTC.2016.7520546.

[16] N. K. Tiwari, S. P. Singh, D. Mondal, and M. J. Akhtar, "Flexible biomedical RF sensors to quantify the purity of medical grade glycerol and glucose concentrations," International Journal of Microwave and Wireless Technologies, vol. 12, no. 2, pp. 120–130, Mar. 2020, doi: 10.1017/S1759078719001089.

[17] C. G. Juan, E. Bronchalo, B. Potelon, C. Quendo, and J. M. Sabater-Navarro, "Glucose Concentration Measurement in Human Blood Plasma Solutions with Microwave Sensors," Sensors, vol. 19, no. 17, Art. no. 17, Jan. 2019, doi: 10.3390/s19173779.

[18] M. Pagnotta, C. L. F. Pooley, B. Gurland, and M. Choi, "Microwave activation of the mutarotation of α-D-glucose: An example of an interinsic microwave effect," Journal of Physical Organic Chemistry, vol. 6, no. 7, pp. 407–411, 1993, doi: 10.1002/poc.610060705.

[19] J. Kim, A. Babajanyan, A. Hovsepyan, K. Lee, and B. Friedman, "Microwave dielectric resonator biosensor for aqueous glucose solution," Review of Scientific Instruments, vol. 79, no. 8, p. 086107, Aug. 2008, doi: 10.1063/1.2968115.

[20] A. Ebrahimi, W. Withayachumnankul, S. F. Al-Sarawi, and D. Abbott, "Microwave microfluidic sensor for determination of glucose concentration in water," in 2015 IEEE 15th Mediterranean Microwave Symposium (MMS), Nov. 2015, pp. 1–3. doi: 10.1109/MMS.2015.7375441.

[21] A. Ebrahimi, J. Scott, and K. Ghorbani, "Microwave reflective biosensor for glucose level detection in aqueous solutions," Sensors and Actuators A: Physical, vol. 301, p. 111662, Jan. 2020, doi: 10.1016/j.sna.2019.111662.

[22] M. F. A. M. Yunos et al., "RF Remote Blood Glucose Sensor and a Microfluidic Vascular Phantom for Sensor Validation," Biosensors, vol. 11, no. 12, Art. no. 12, Dec. 2021, doi: 10.3390/bios11120494.

[23] T. Yilmaz, R. Foster, and Y. Hao, "Towards Accurate Dielectric Property Retrieval of Biological Tissues for Blood Glucose Monitoring," IEEE Transactions on Microwave Theory and Techniques, vol. 62, no. 12, pp. 3193–3204, Dec. 2014, doi: 10.1109/TMTT.2014.2365019.

[24] R. J. Buford, E. C. Green, and M. J. McClung, "A microwave frequency sensor for non-invasive blood-glucose measurement," in 2008 IEEE Sensors Applications Symposium, Feb. 2008, pp. 4–7. doi: 10.1109/SAS.2008.4472932.

[25] V. Turgul and I. Kale, "A novel pressure sensing circuit for non-invasive RF/microwave blood glucose sensors," in 2016 16th Mediterranean Microwave Symposium (MMS), Nov. 2016, pp. 1–4. doi: 10.1109/MMS.2016.7803818.

[26] N. Y. Kim, R. Dhakal, K. K. Adhikari, E. S. Kim, and C. Wang, "A reusable robust radio frequency biosensor using microwave resonator by integrated passive device technology for quantitative detection of glucose level," Biosensors and Bioelectronics, vol. 67, pp. 687–693, May 2015, doi: 10.1016/j.bios.2014.10.021.

[27] A. Moreno-Oyervides et al., "Early, Non-Invasive Sensing of Sustained Hyperglycemia in Mice Using Millimeter-Wave Spectroscopy," Sensors, vol. 19, no. 15, Art. no. 15, Jan. 2019, doi: 10.3390/s19153347.

[28] A. E. Omer et al., "Low-cost portable microwave sensor for non-invasive monitoring of blood glucose level: novel design utilizing a four-cell CSRR hexagonal configuration," Sci Rep, vol. 10, no. 1, Art. no. 1, Sep. 2020, doi: 10.1038/s41598-020-72114-3.

[29] H. Choi, S. Luzio, J. Beutler, and A. Porch, "Microwave noninvasive blood glucose monitoring sensor: Human clinical trial results," in 2017 IEEE MTT-S International Microwave Symposium (IMS), Jun. 2017, pp. 876–879. doi: 10.1109/MWSYM.2017.8058721.

[30] J. Hanna et al., "Noninvasive, wearable, and tunable electromagnetic multisensing system for continuous glucose monitoring, mimicking vasculature anatomy," Sci Adv, vol. 6, no. 24, p. eaba5320, Jun. 2020, doi: 10.1126/sciadv.aba5320.

[31] K. Kwon et al., "Planar type probe with multiple-polarization response for in-vivo permittivity measurements of heterogeneous biological tissues," Microwave and Wireless Components Letters, IEEE, vol. 16, pp. 1–3, Feb. 2006, doi: 10.1109/LMWC.2005.861364.

[32] R. Zhang et al., "Noninvasive Electromagnetic Wave Sensing of Glucose," Sensors, vol. 19, no. 5, Art. no. 5, Jan. 2019, doi: 10.3390/s19051151.

[33] T. Yilmaz, R. Foster, and Y. Hao, "Radio-Frequency and Microwave Techniques for Non-Invasive Measurement of Blood Glucose Levels," Diagnostics, vol. 9, no. 1, Art. no. 1, Mar. 2019, doi: 10.3390/diagnostics9010006.

[34] R. J, R. S, G. A, and W. Wk, "Predictive monitoring for improved management of glucose levels," Journal of diabetes science and technology, vol. 1, no. 4, Jul. 2007, doi: 10.1177/193229680700100405.

[35] C. Pérez-Gandía et al., "Artificial neural network algorithm for online glucose prediction from continuous glucose monitoring," Diabetes Technol Ther, vol. 12, no. 1, pp. 81–88, Jan. 2010, doi: 10.1089/dia.2009.0076.

[36] X. Lu and R. Song, "A Hybrid Deep Learning Model for the Blood Glucose Prediction," in 2022 IEEE 11th Data Driven Control and Learning Systems Conference (DDCLS), Aug. 2022, pp. 1037–1043. doi: 10.1109/DDCLS55054.2022.9858348.

[37] J. Daniels, P. Herrero, and P. Georgiou, "A Multitask Learning Approach to Personalized Blood Glucose Prediction," IEEE J Biomed Health Inform, vol. 26, no. 1, pp. 436–445, Jan. 2022, doi: 10.1109/JBHI.2021.3100558.

[38] T. Hamdi, J. Ben Ali, V. Di Costanzo, F. Fnaiech, E. Moreau, and J.-M. Ginoux, "Accurate prediction of continuous blood glucose based on support vector regression and differential evolution algorithm," Biocybernetics and Biomedical Engineering, vol. 38, no. 2, pp. 362–372, Jan. 2018, doi: 10.1016/j.bbe.2018.02.005.

[39] G. Alfian, M. Syafrudin, J. Rhee, M. Anshari, M. Mustakim, and I. Fahrurrozi, "Blood Glucose Prediction Model for Type 1 Diabetes based on Extreme Gradient Boosting," IOP Conf. Ser.: Mater. Sci. Eng., vol. 803, no. 1, p. 012012, Apr. 2020, doi: 10.1088/1757-899X/803/1/012012.

[40] H. Nemat, H. Khadem, M. R. Eissa, J. Elliott, and M. Benaissa, "Blood Glucose Level Prediction: Advanced Deep-Ensemble Learning Approach," IEEE Journal of Biomedical and Health Informatics, vol. 26, no. 6, pp. 2758–2769, Jun. 2022, doi: 10.1109/JBHI.2022.3144870.

[41] "47 CFR 1.1310 -- Radiofrequency radiation exposure limits." https://www.ecfr.gov/current/title-47/chapter-I/subchapter-A/part-1/subpart-I/section-1.1310 (accessed Feb. 14, 2023).

[42] E. Bingham and H. Mannila, "Random projection in dimensionality reduction: applications to image and text data," in Proceedings of the seventh ACM SIGKDD international conference on Knowledge discovery and data mining, in KDD '01. New York, NY, USA: Association for Computing Machinery, Aug. 2001, pp. 245–250. doi: 10.1145/502512.502546.

[43] S. Dasgupta, "Experiments with Random Projection," Jan. 2013, doi: 10.48550/arXiv.1301.3849.